

# LPLI Inhibits Apoptosis Upstream of Bax Translocation via a GSK-3 $\beta$ -Inactivation Mechanism

LINGLING ZHANG, YINGJIE ZHANG, AND DA XING\*

MOE Key Laboratory of Laser Life Science & Institute of Laser Life Science, College of Biophotonics, South China Normal University, Guangzhou, China

Low-power laser irradiation (LPLI), a non-damage physical therapy, which has been used clinically for decades of years, is shown to promote cell proliferation and prevent apoptosis. However, the underlying mechanisms that LPLI prevents cell apoptosis remain undefined. In this study, based on real-time single-cell analysis, we demonstrated for the first time that LPLI inhibits staurosporine (STS)-induced cell apoptosis by inactivating the GSK-3 $\beta$ /Bax pathway. LPLI could inhibit the activation of GSK-3 $\beta$ , Bax, and caspase-3 induced by STS. In the searching for the mechanism, we found that, LPLI can activate Akt, which was consistent with our former research, even in the presence of STS. In this anti-apoptotic process, the interaction between Akt and GSK-3 $\beta$  increased gradually, indicating Akt interacts with and inactivates GSK-3 $\beta$  directly. Conversely, LPLI decreased the interaction between GSK-3 $\beta$  and Bax, with the suppression of Bax translocation to mitochondria, suggesting LPLI inhibits Bax translocation through inactivating GSK-3 $\beta$ . These results were further confirmed by the experiments of co-immunoprecipitation. Wortmannin, an inhibitor of phosphatidylinositol 3'-OH kinase (PI3K), potently suppressed the activation of Akt and subsequent anti-apoptotic processes induced by LPLI. Taken together, we conclude that LPLI protects against STS-induced apoptosis upstream of Bax translocation via the PI3K/Akt/GSK-3 $\beta$  pathway. These findings raise the possibility of LPLI as a promising therapy for neuron-degeneration disease induced by GSK-3 $\beta$ .

J. Cell. Physiol. 224: 218–228, 2010. © 2010 Wiley-Liss, Inc.

Low-power laser irradiation (LPLI) has been used clinically to accelerate wound healing (Conlan et al., 1996) and reduce pain (Chow and Barnsley, 2005) and inflammation in a variety of pathologies (Amano et al., 1994; Schindl et al., 1999; Bjordal et al., 2003, 2006; Hirschl et al., 2004; Mizutani et al., 2004), but the biological mechanisms behind observed beneficial results in clinical trials remain unclear. In vitro, many studies have demonstrated that LPLI can modulate various biological processes including cell growth, proliferation, and differentiation (Yu et al., 1996; Ben-Dov et al., 1999; Shefer et al., 2001; Gao et al., 2006; Zhang et al., 2008a). In recent years, accumulating research suggests that LPLI could inhibit apoptosis and promote cell survival. They discovered that LPLI could rescue cells from multiple apoptotic stimuli, such as A $\beta$  (Zhang et al., 2008b) and serum withdrawal (Shefer et al., 2002). However, the underlying molecular mechanisms are not understood. One possibility is that mitochondrial respiration or redox status is involved in LPLI-induced cell survival, since LPLI treatment is well known to increase in mitochondrial respiration and ATP synthesis (Tafur and Mills, 2008; Silveira et al., 2009). Apoptosis, as we all know, contributes to a variety of diseases and injury (Bennett, 2002; Kang and Izumo, 2003). Staurosporine (STS) is widely employed as an inducer of apoptosis in many cell types (Stepczynska et al., 2001). We have shown that LPLI triggers a significant activation of phosphatidylinositol 3'-OH kinase (PI3K)/Akt pathway (Zhang et al., 2009a). Besides, active Akt protects cells from apoptotic in response to STS (Mookherjee et al., 2007).

Akt is a serine/threonine protein kinase that has been implicated in mediating distinct biological responses, including promoting proliferation and inhibiting apoptosis (Dudek et al., 1997; Cardone et al., 1998; Brunet et al., 1999; Lawlor and Alessi, 2001). Growing evidence indicates that Akt is a critical mediator of survival signals that protect cells from different apoptotic stimuli such as growth factor withdrawal, UV irradiation and cell-cycle discordance (Kauffmann-Zeh et al., 1997; Kennedy et al., 1997; Khwaja et al., 1997; Chen et al.,

1998; Crowder and Freeman, 1998). Its activity is positively regulated by phosphorylation on residues Thr308 and Ser473 downstream of PI3-kinase (Alessi et al., 1996). Once activated, Akt exerts anti-apoptotic effects by both impinging on the cytoplasmic cell death machinery and by regulating the expression of genes involved in cell death and survival. Akt inhibits the activity of transcription factors FOXO (Brunet et al., 1999) and p53 (Yamaguchi et al., 2001), thereby preventing the expression of their target death genes. Akt also activates NF- $\kappa$ B indirectly (Ozes et al., 1999), leading to the expression of survival genes, such as *a1*, *bcl-xL*, and *iap*. In addition, Akt phosphorylates and inhibits some pro-apoptotic

**Abbreviations:** CCK-8, Cell Counting Kit-8; CFP, GFP, and YFP, cyan, green, and yellow fluorescent protein; FRET, fluorescence resonance energy transfer; GSK-3 $\beta$ , glycogen synthase kinase-3 $\beta$ ; LPLI, low-power laser irradiation; PI3K, phosphoinositide 3-kinase; STS, staurosporine.

Contract grant sponsor: National Basic Research Program of China;  
Contract grant number: 2010CB732602.  
Contract grant sponsor: Program for Changjiang Scholars and Innovative Research Team in University;  
Contract grant number: IRT0829.  
Contract grant sponsor: National Natural Science Foundation of China;  
Contract grant numbers: 30870676, 30870658.

\*Correspondence to: Da Xing, MOE Key Laboratory of Laser Life Science & Institute of Laser Life Science, College of Biophotonics, South China Normal University, Guangzhou 510631, China.  
E-mail: xingda@scnu.edu.cn

Received 10 November 2009; Accepted 27 January 2010

Published online in Wiley InterScience  
(www.interscience.wiley.com.), 23 March 2010.  
DOI: 10.1002/jcp.22123

proteins activity, including Bad (Datta et al., 1997) and ASK1 (Kim et al., 2001), to promote survival. Importantly, Akt phosphorylating and inhibiting glycogen synthase kinase-3 $\beta$  (GSK-3 $\beta$ ) has also been suggested to play a significant role in inhibiting apoptosis (Cross et al., 1995, 2000).

Glycogen synthase kinase-3 $\beta$  (GSK-3 $\beta$ ) is a critical activator of apoptosis induced by a diverse array of toxicity insults, including STS and heat shock (Bijur et al., 2000). Isolated studies have identified a specific role for GSK-3 $\beta$  in the p53 response: promoting p53-dependent apoptosis (Wacharasit et al., 2003) and regulating endoplasmic reticulum stress-mediated p53 activation (Qu et al., 2004). Currently, there is evidence suggests GSK-3 $\beta$  exerts some of its pro-apoptotic effects by regulating the mitochondrial localization of Bax (Linseman et al., 2004), a key component of the intrinsic apoptotic cascade. However, the mechanism of GSK-3 $\beta$  regulating Bax is still controversial.

As Bcl-2 family members act upstream of irreversible cellular damage to regulate the mitochondrial pathway to apoptosis, they play a pivotal role in deciding whether a cell will live or die. Bax, an essential regulator of the mitochondrial pathway of apoptosis (Wei et al., 2001), is normally found in the cytosol of healthy cells and translocates to the mitochondria during apoptosis (Hsu et al., 1997). Resent studies support a model in which the activation of Bax by BH3-only "activator" proteins and, perhaps, other proteins (such as p53) with this activator function. This effect is regulated by anti-apoptotic members of the Bcl-2 family that can sequester the activator protein and also bind to activated Bax to inhibit their ability to oligomerize and permeabilize membranes. It was also reported that the transcription independent activation of Bax by active GSK-3 $\beta$  occurred with similar kinetics and concentrations to those produced by p53 (Tan et al., 2005).

Our previous studies demonstrated that PI3K/Akt signaling pathway is activated during LPLI-induced proliferation (Zhang et al., 2009a). However, whether PI3K/Akt pathway is activated in the presence of STS and how to exert its anti-apoptotic function is unclear. In order to enunciate it, based on real-time single-cell analysis, we found that LPLI could suppress Bax translocation and caspase-3 activation, and then inhibit apoptosis. Specifically, we investigated the activation of Akt, and the interaction among Akt, GSK-3 $\beta$ , and Bax during LPLI-mediated cell protection against STS. We found that LPLI suppresses Bax translocation through PI3K/Akt/GSK-3 $\beta$  pathway.

## Materials and Methods

### Chemicals

Dulbecco's modified Eagle's medium (DMEM) was purchased from GIBCO (Grand Island, NY). STS and epidermal growth factor (EGF) (diluted in DMSO) were purchased from PeproTech (Rocky Hill, NJ). Hoechst 33258 was purchased from Sigma Chemical Co. (St. Louis, MO). Wortmannin and LiCl were purchased from BIOMOL Research Laboratories, Inc. (Plymouth, PA). All the antibodies were purchased from Cell Signaling (Beverly, MA). Cell Counting Kit-8 (CCK-8) was purchased from Dojindo Laboratories (Kumamoto, Japan). Lipofectamine™ Reagent was purchased from Invitrogen (Carlsbad, CA). DNA extraction kit was purchased from Qiagen (Valencia, CA). Other chemicals were mainly from Sigma Chemical Co. The concentrations of STS, EGF, wortmannin, and LiCl used in our experiments were 1  $\mu$ M, 50 ng/ml, 1  $\mu$ M, and 10 mM, respectively.

### Cell culture and transfection

The human lung adenocarcinoma cell line (ASTC-a-1) was obtained from Department of Medicine, Jinan University. The cells were cultured in DMEM supplemented with 15% fetal calf serum (FCS),

penicillin (100 units/ml), and streptomycin (100 mg/ml) in 5% CO<sub>2</sub> at 37°C in humidified incubator. The medium was refreshed every other day, and the cells were plated at appropriate densities according to each experimental protocol. Before transfection, the cells were cultured in a custom-built dish. When the cells came to 70–80% confluence, transfections were performed with 1  $\mu$ g of expression vectors using the Lipofectamine™ 2000 reagent according to the manufacturer's protocol in serum-free medium. The medium was replaced with fresh culture medium after 5 h. Cells were examined at 24–48 h after transfection.

B kinase activity reporter (BKAR, a kind gift from Dr. Newton, University of California, San Diego) was used to monitor Akt activity. It consists of mCFP (cyan fluorescent protein), the FHA2 domain of Rad53p, a consensus Akt phosphorylation sequence and mYFP (yellow fluorescent protein) (Kunkel et al., 2005). The ratio of fluorescence resonance energy transfer (FRET)/CFP decreases with the activation of Akt as it is described before (Zhang et al., 2009a). Another genetic reporter, SCAT3, (a kind gift from Dr. Miura, RIKEN Brain Science Institute, Japan) was used to monitor caspase-3 activity. The working mechanism of SCAT3 is shown in Figure 1. This reporter consists of a donor cyan fluorescent protein (CFP) and an acceptor Venus (a mutant of yellow fluorescent protein). The donor and the acceptor are linked with a caspase-3 recognition and cleavage sequence (DEVD) (Takemoto et al., 2003). Activation of caspase-3 leads to the cleavage of the linker, thus effectively reducing the FRET. Therefore, a decrease in the FRET represents activation of the caspase-3. The cells stably expressing SCAT3 reporter were screened with 0.8 mg/ml G418, and positive clones were picked up with micropipettes. pEGFP-Akt was kindly supplied by Dr. Badger (He et al., 2006). pYFP-GSK-3 $\beta$  was kindly supplied by Dr. Kehrl (Shi et al., 2006). pGFP-Bax was kindly supplied by Dr. Youle (Nechushtan et al., 1999). pDsRed-Mit was kindly supplied by Dr. Gotoh (Tsuruta et al., 2002).

For Bax gene silencing by siRNA, RNA interference of Bax was performed using 24-bp small interfering RNA (siRNA) duplexes purchased from Gene Pharma (Shanghai, China). The sense strand nucleotide sequence for Bax siRNA was AACATGGAGCT-GCAGAGGATGAdTdT. A control siRNA specific to the GFP DNA sequence CCACTACCTGAGCACCCAG was used as a negative control. After transfection and expression, the protein levels of Bax were detected in the cell lysate by Western blot.

### Low-power laser irradiation

ASTC-a-1 cells (monolayer cells at a density of  $1 \times 10^6$  cells/dish) cultured for 24 h were treated with different chemicals and/or irradiated with He-Ne laser (632.8 nm, 10 mW, 12.74 mW/cm<sup>2</sup>, HN-1000, Guangzhou, China) at a fluence of 1.2 J/cm<sup>2</sup>. The chemicals were added to the culture medium 30 min before LPLI treatment. The entire procedure was carried out at room

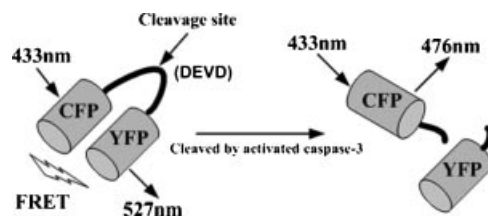


**Fig. 1.** Schematic representation of SCAT-3. SCAT-3, a caspase-3 activity reporter, consists of a donor CFP and an acceptor Venus. The donor and the acceptor are linked with a caspase-3 recognition and cleavage sequence (DEVD). The activation of caspase-3 leads to the cleavage of the linker, thus effectively reducing the FRET. Since it does not contain the full caspase-3 sequence, but a caspase-3 substrate, it monitors the activation of endogenous caspase-3 in live cells.

temperature. Throughout each experiment, the cells were kept either in a complete dark or a very dim environment, except when subjected to the light irradiation, to minimize the ambient light interference.

#### Cell viability and apoptosis assays

ASTC-a-1 cells were cultured in 96-well microplate at a density of  $5 \times 10^3$  cells/well for 24 h. The cells were then divided into five groups and exposed to He-Ne laser irradiation at fluence of 0, 0.4, 0.8, 1.2, and 2.4 J/cm<sup>2</sup> plus 1  $\mu$ M STS, respectively. Another group was pre-treated with wortmannin and then exposed to 1  $\mu$ M STS plus 2.4 J/cm<sup>2</sup> LPLI. The irradiation was performed on monolayer cells. In all cases, control (non-irradiated) cells were kept in the same conditions as the treated cells. Cell viability was assessed with CCK-8 (Dojindo Laboratories) at 6 h post-treatment according to the manufacturer's instructions. OD450, the absorbance value at 450 nm, was read with a 96-well plate reader (DG5032, Hua dong, Nanjing, China), to determine the viability of the cells.

For analysis of apoptosis by nuclear staining, cell apoptosis was morphologically evaluated with Hoechst 33258. ASTC-a-1 cells were treated as indicated and incubated for 6 h in 35 mm dish. Hoechst 33258 (10  $\mu$ g/ml) was added to each dish and the cells were incubated at 37°C with 5% CO<sub>2</sub> for an additional 30 min in the dark. Fluorescence images of the normal and apoptotic cells were examined with a modified commercial microscope system equipped with a mercury lamp (band-pass filter: 352–461 nm), a 395 nm dichroic mirror and a long-pass filter 397 nm emission filter (LSM510/ConfoCor2, Zeiss, Jena, Germany). The fluorescence images were collected via a Zeiss C-Apochromat objective (40 $\times$ , NA = 1.3).

#### Time-lapse confocal fluorescence microscopy

GFP, CFP, YFP, DsRed, and MitoTracker fluorescence were monitored confocally using a commercial laser scanning microscope (LSM 510/ConfoCor 2) combination system (Zeiss) equipped with a Plan-Neofluar 40  $\times$  /1.3 NA Oil DIC objective. Excitation wavelength and detection filter settings for each of the fluorescent indicators were as follows: GFP fluorescence was excited at 488 nm with an argon ion laser and emission was recorded through a 500–520 nm band pass filter. CFP fluorescence was excited at 458 nm with an argon ion laser and emission was recorded through a 470–500 nm band pass filter. YFP fluorescence was excited at 514 nm with an argon ion laser and emission was recorded through a 535–545 nm band pass filter. DsRed-Mit fluorescence was excited at 543 nm with a helium-neon laser and emitted light was recorded through a 560 nm long pass filter. MitoTracker fluorescence was excited at 633 nm with a helium-neon laser and emitted light was recorded through a 650 nm long pass filter.

For time-lapse imaging, culture dishes were mounted onto the microscope stage that was equipped with a temperature-controlled chamber (Zeiss). During control experiments, bleaching of the probe was negligible.

#### GFP-Bax translocation assay

To monitor GFP-Bax translocation in living cells, ASTC-a-1 cells were co-transfected with pGFP-Bax and pDsRed-Mit. Using Zeiss LSM 510 confocal microscope, we imaged both the distribution pattern of GFP-Bax and that of DsRed-Mit simultaneously after different treatments. Bax redistribution was assessed by the matching fluorescence of GFP-Bax and DsRed-Mit emission. The cells exhibiting strong punctate staining of GFP, which overlapped with the distribution of DsRed, were counted as the cells with mitochondrially localized Bax.

#### FRET analysis

FRET was performed on a commercial Laser Scanning Microscopes (LSM510/ConfoCor2) combination system (Zeiss). For excitation,

the 458 nm line of an Ar-ion laser was attenuated with an acousto-optical tunable filter, reflected by a dichroic mirror (main beam splitter HFT458), and focused through a Zeiss Plan-Neofluar 40 $\times$ /1.3 NA Oil Dic objective onto the sample. CFP and YFP (FRET acceptor) emission were collected through 470–500 and 535–545 nm band pass filters, respectively. GFP and YFP (FRET donor) emission were collected through 500–520 and 535–545 nm band pass filters, respectively. The quantitative analysis of the fluorescence images was performed using Zeiss Rel3.2 image processing software (Zeiss). After background subtraction, the average fluorescence intensity per pixel was calculated. During control experiments, bleaching of the probe was negligible.

#### Western blot analysis and co-immunoprecipitation

At the indicated time after different treatments, cells were scraped from the dish, then washed twice with ice-cold phosphate-buffered saline (PBS, pH 7.4), and lysed with ice-cold lysis buffer (50 mmol/L Tris-HCl pH 8.0, 150 mmol/L NaCl, 1% Triton X-100, 100  $\mu$ g/ml PMSF) for 30 min on ice. The lysates were centrifuged at 12,000 rpm for 5 min at 4°C, and the protein concentration was determined. Equivalent samples were subjected to SDS-PAGE on 12% gel. The proteins were then transferred onto nitrocellulose membranes, and probed with indicated primary antibody, followed by secondary antibodies: goat anti-mouse conjugated to Alexa Fluor 680 or goat anti-rabbit conjugated to IRDyeTM800. Detection was performed using the LI-COR Odyssey Infrared Imaging System (LI-COR, Inc. Lincoln, Nebraska).

For immunoprecipitation (IP), about 4  $\mu$ l of IP antibodies were added to 400  $\mu$ l cell lysates. The mixtures were mixed on a rocker at ambient temperature for 2 h. The immunocomplexes were captured by the addition of protein G/A-agarose (Roche Applied Sciences, Indianapolis, IN 46250-0414) mixed at 1:10 ratio, followed by incubation at ambient temperature for 1 h. The beads were washed three times by PBS and then collected by centrifugation at 12,000 rpm for 5 sec. After the final wash, the beads were mixed with 60  $\mu$ l of 2 $\times$  Laemmli sample buffer, heated at 100°C for 5 min, and analyzed by Western blot.

#### Flow cytometry

For flow cytometric analysis (FACS analysis), Annexin-V-FITC conjugate and binding buffer were used as standard reagents. Flow cytometry was performed on a FACScanto flow cytometer (Becton Dickinson, Mountain View, CA) with excitation at 488 nm. Fluorescent emission of FITC was measured at 515–545 nm and that of DNA-PI complexes at 564–606 nm. Cell debris was excluded from analysis by an appropriate forward light scatter threshold setting. Compensation was used wherever necessary.

#### Statistics analysis

All assays were repeated independently for a minimum of three times. Data represent the mean  $\pm$  SEM. Statistical analysis was performed with Student's paired *t*-test. Differences were considered statistically significant at  $P < 0.05$ .

## Results

### LPLI prevents cell apoptosis induced by STS

To establish a proper laser irradiation dose to protect cell from apoptosis, ASTC-a-1 cells were treated with different doses of laser irradiation after STS stimulation. Cell viability was analyzed using CCK-8 assay 6 h after STS stimulation. As shown in Figure 2A, the cell viability significantly decreased in cells treated with STS compared with that of non-treated cells. While, after LPLI stimulation, cells were found to be more resistant to STS. Wortmannin, an inhibitor of PI3K, could abolish this effect of LPLI. These results indicate that, in the range 0.8–2.4 J/cm<sup>2</sup>, laser irradiation has a promotive effect on cell survival, which is dependent on PI3K activity. Therefore,

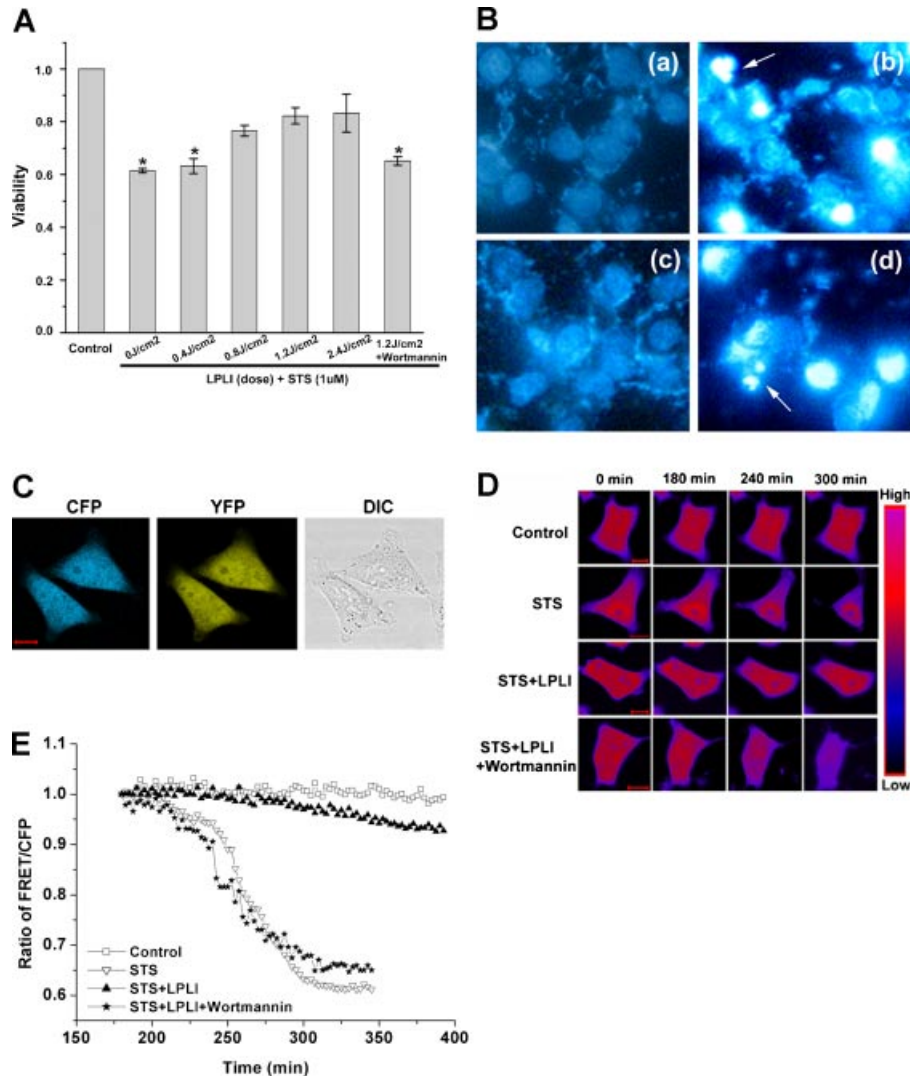


**Fig. 2.** Effects of LPLI on STS-induced cell apoptosis. **A:** Cell viability measured with CCK8 assay. Error bars are SEM from four independent experiments; \* $P < 0.05$ . **B:** Hoechst 33258 morphological examination of LPLI inhibiting apoptosis. (a) Normal culture condition. (b) Cells treated with 1  $\mu\text{mol/L}$  STS for 6 h. (c) Cells treated with STS (1  $\mu\text{M}$ ) plus LPLI (1.2 J/cm<sup>2</sup>) for 6 h. (d) Cells pretreated with wortmannin (1  $\mu\text{M}$ ) for 30 min before and during the co-application of STS and LPLI. Condensation fragmentation (as the arrow indicates). **C–E:** Single-cell imaging analysis of caspase-3 activity in SCAT3-expressing living cells. **C:** The fluorescence images of CFP and FRET channels and the DOI image in cells stably expressing SCAT-3 reporter. **D:** Representative pseudocolor imaging series of FRET/CFP ratios after various treatments. Scale bar: 10  $\mu\text{m}$ . **E:** Quantitative analysis of FRET/CFP ratio corresponding to the images in **D**. The FRET/CFP ratios at the first time point are normalized to 1. [Color figure can be viewed in the online issue, which is available at [www.interscience.wiley.com](http://www.interscience.wiley.com).]

in our following experiments, we selected 1.2 J/cm<sup>2</sup> as the irradiation dose.

To observe the status of cell apoptosis directly, morphological examination was performed with Hoechst 33258 staining. As shown in Figure 2B, chromatin condensation was observed 6 h after cells exposure to STS, indicating the occurrence of apoptosis. The nuclei of cells treated with STS plus LPLI show no difference with that of the control. Wortmannin could remove the role of LPLI in protection against apoptosis. These results further confirm that LPLI could inhibit STS-induced cell apoptosis, which is dependent on PI3K.

Caspase activation is an important event in mitochondrial apoptosis pathway. The effector caspases-3 can disrupt entire cells within a few minutes (Earnshaw et al., 1999). The mechanism that STS induces apoptosis, especially whether caspase is involved in is still controversial (Deas et al., 1998; Tafani et al., 2002). To clarify this conflict, the activity of

caspase-3 in single living cell that expressing SCAT 3 reporters (Fig. 2C) was monitored by FRET technique. The typical time-course images of the pseudocolor images for the ratio of FRET/CFP fluorescence are shown in Figure 2D. The ratio of FRET/CFP emission decreased significantly in cells subjected to STS, indicating the activation of caspase-3. However, the ratio remained almost unchanged in cells treated with STS plus LPLI, indicating that LPLI can inhibit STS-induced caspase-3 activation. Similarly, the effect of LPLI was abolished by wortmannin. The result was further confirmed by the statistical analysis of fluorescence intensities (Fig. 2E).

#### Real-time monitoring of Akt activation in single living cell

Since we have confirmed that the anti-apoptotic effect of LPLI is dependent on PI3K, the PI3K/Akt pathway may be involved in

this process. To further determine it, the effects of LPLI on Akt activation in cells expressing pBKAR were monitored by FRET technique. The decrease of FRET/CFP ratio represents the activation of Akt as it is described in the method. The fluorescence images of CFP, FRET and the ratio of FRET/CFP after  $1.2 \text{ J/cm}^2$  LPLI treatment are shown in Figure 3A. The results show that with the passage of time, the CFP fluorescence increased, while the FRET fluorescence and the FRET/CFP ratio decreased, indicating the activation of Akt. Figure 3B was the quantitative analysis of FRET/CFP ratio after various stimulations. The ratio decreased when the cells were subject to LPLI, even in the presence of STS. The decreased trend of the ratio was reversed in response to wortmannin exposure. These indicate that LPLI could effectively activate Akt even in cells exposed to STS, and this activation is dependent on PI3K activity. The results were also confirmed by Western blot analysis (Fig. 3C).

### LPLI inhibits STS-induced Bax translocation

Previous studies have demonstrated that Bax translocation is involved in the process of STS-induced apoptosis (Tsuruta et al., 2002). These prompted us to investigate whether LPLI exerts its anti-apoptotic effect through suppressing Bax activation. To clarify it, real-time monitoring of GFP-Bax translocation from the cytosol to the mitochondria was performed. ASTC-a-1 cells were transiently co-transfected with GFP-Bax and DsRed-Mit (a marker for mitochondria), followed by different treatments as indicated. As shown in Figure 4B, GFP-Bax translocated in typical cells at about 4 h after STS treatment. While when the cells were treated with STS plus LPLI, GFP-Bax remained diffusion in the

whole cell as that of the control (Fig. 4A), except for some cell deformation, for more than 7 h (Fig. 4C). These indicate that LPLI could inhibit Bax translocation induced by STS.

Then, wortmannin or LiCl was added 30 min before treatment. As shown in Figure 4D, GFP-Bax translocated to mitochondria at about 4.5 h in the presence of wortmannin. This indicates that LPLI suppresses Bax translocation through activating PI3K/Akt pathway. However, when cells exposed to STS in the presence of LiCl, there was no significant difference in temporal and spatial redistribution of GFP-Bax as compared to Figure 4C (Fig. 4E). That means inhibiting the activity of GSK-3 $\beta$  could suppress Bax translocation as LPLI did, indicating GSK-3 $\beta$  plays an important role in STS-induced Bax translocation. Taken together, these results demonstrate that LPLI suppresses Bax translocation through inactivating GSK-3 $\beta$ , which is dependent on PI3K/Akt activation. The results were further confirmed by the statistical analysis (Fig. 4F).

### Akt interacts with and inactivates GSK-3 $\beta$ during LPLI mediated protection against apoptosis

In order to further confirm our hypothesis that LPLI protects cell from STS-induced apoptosis through inactivating GSK-3 $\beta$ , we studied the actions of GSK-3 $\beta$  and its interaction with Akt. The mechanisms controlling the actions of GSK-3 $\beta$ , involves phosphorylation, distribution and protein complexes. Firstly, the distribution of GSK-3 $\beta$  was detected by using fluorescence imaging. ASTC-a-1 cells transiently transfected with YFP-GSK-3 $\beta$  were stimulated with different treatments as indicated, then performed with the LSM microscope. The nuclear translocation indicates the activation of GSK-3 $\beta$ . As LiCl is the

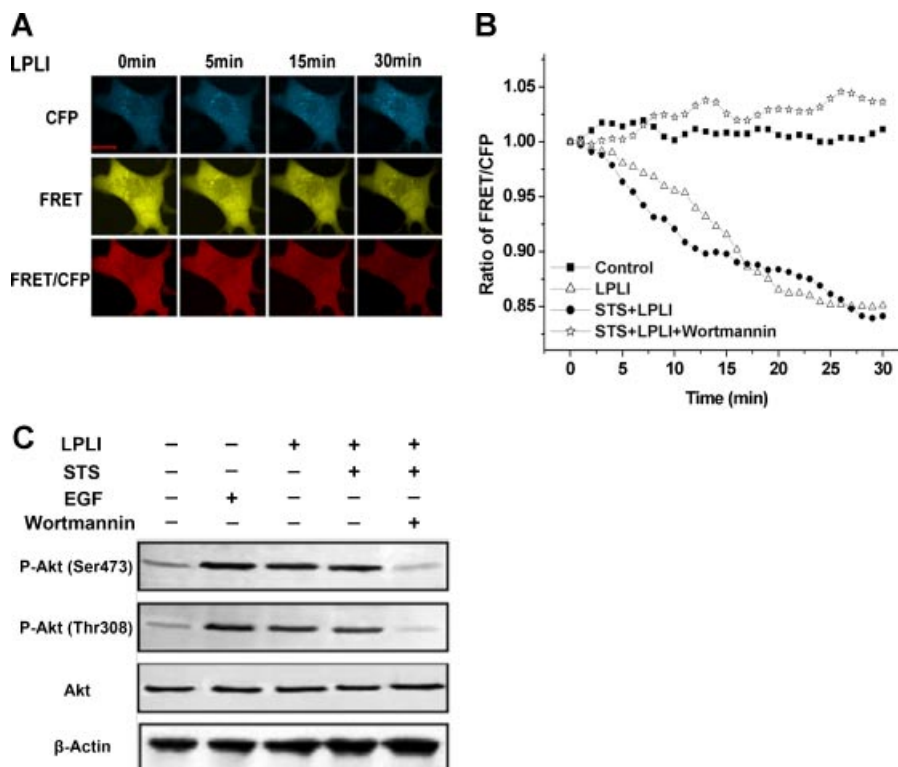


**Fig. 3. Akt activation induced by LPLI. A,B:** Single-cell imaging analysis of ASTC-a-1 cells transfected with BKAR in different conditions. **A:** Representative fluorescence images of CFP, FRET, and FRET/CFP ratio after  $1.2 \text{ J/cm}^2$  LPLI treatment in single ASTC-a-1 cell. Scale bar:  $10 \mu\text{m}$ . **B:** Quantitative analysis of FRET/CFP ratio corresponding to the images in A. **C:** Western blot analysis for Akt Thr308 and Ser473 phosphorylation. Akt and  $\beta$ -actin were used as a loading control. Results represent one of three replicates. [Color figure can be viewed in the online issue, which is available at [www.interscience.wiley.com](http://www.interscience.wiley.com).]

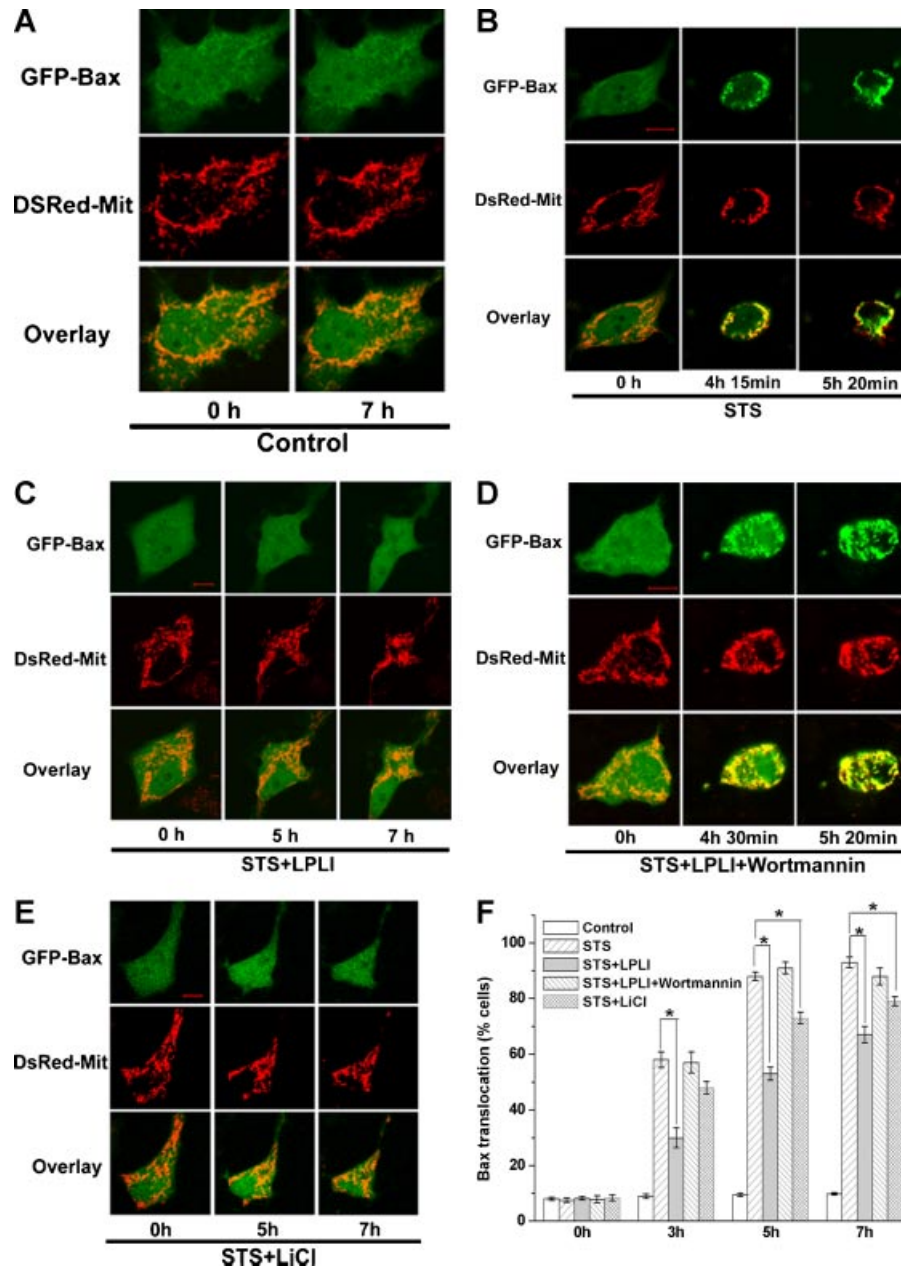


**Fig. 4.** Bax translocation induced by STS was inhibited by LPLI. **A–E:** Dynamics of GFP-Bax translocation in various conditions. ASTC-a-1 cells co-transfected with GFP-Bax and DsRed-Mit were **A:** untreated or treated with **B:** STS, **C:** STS plus 1.2 J/cm<sup>2</sup> LPLI, **D:** STS plus 1.2 J/cm<sup>2</sup> LPLI in the presence of wortmannin, **E:** STS plus LiCl. The two parts of GFP-Bax and DsRed-Mit are shown separately and are merged to show the overlay. GFP-Bax localization at mitochondria was determined based on the overlap of GFP-Bax and DsRed-Mit fluorescence images. Scale bar: 10  $\mu$ m. **F:** Quantification of cells showing mitochondrial GFP-Bax. At the indicated time points, the percentage of cells showing Bax translocation to mitochondria was assessed by counting the number of cells. Data were collected from  $n = 150$ –200 cells per treatment in 10–15 randomly selected image frames from three independent experiments. Data represent the mean  $\pm$  SEM; \* $P < 0.05$ . [Color figure can be viewed in the online issue, which is available at [www.interscience.wiley.com](http://www.interscience.wiley.com).]

inhibitor of GSK-3 $\beta$ , we used the group of STS plus LiCl as the negative control. The results show that there is a significant nuclear translocation at about 30 min after STS treatment, which was inhibited by LPLI. While, wortmannin reversed the inhibition of LPLI evidently (Fig. 5A).

Next, Western blot analysis was used to detect the phosphorylation of GSK-3 $\beta$ . GSK-3 $\beta$  is inactive when its Ser-9 is phosphorylated. As shown in Figure 5B, compared with that of non-treated cells, the phosphorylation level of GSK-3 $\beta$  elevated in cells treated with LPLI. While in the cells treated

with STS only or in the presence of wortmannin, the phosphorylation level is lower than that of the control. These results are consistent with our former experiments and further demonstrate that, GSK-3 $\beta$  is activated in response to STS, while LPLI could inactivate it in a PI3K/Akt-dependent manner.

Finally, we investigated the dynamic interaction between Akt and GSK-3 $\beta$ . ASTC-a-1 cells were transiently co-transfected with GFP-Akt and YFP-GSK-3 $\beta$ , followed with the treatments of STS and 1.2 J/cm<sup>2</sup> LPLI in the presence or absence of wortmannin. The fluorescence images of GFP, FRET and the

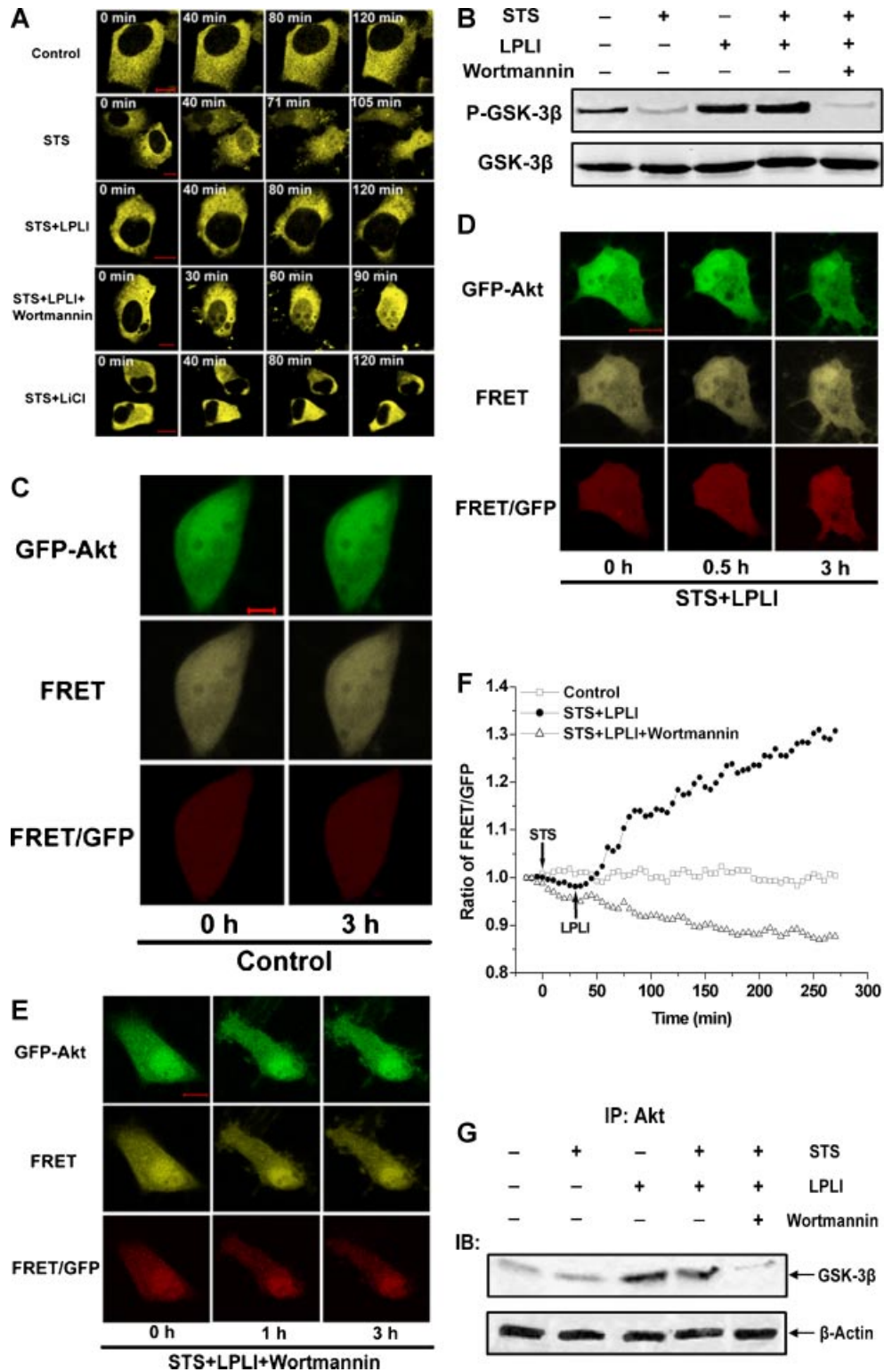


**Fig. 5.** Akt interacted and inactivated GSK-3 $\beta$  directly after LPLI treatment. **A,B:** GSK-3 $\beta$  was inactivated after 1.2 J/cm<sup>2</sup> LPLI treatment in cells exposed to STS. **A:** Dynamics of YFP-GSK-3 $\beta$  nuclear translocation in different conditions. LiCl was used as a negative control. **B:** Western blot analysis for GSK-3 $\beta$  phosphorylation. Results represent one of three replicates. **C–F:** Single-cell imaging analysis of the interaction between GFP-Akt and YFP-GSK-3 $\beta$ . **C:** Typical fluorescence images of GFP, FRET, and FRET/GFP ratio in untreated cell. **D:** Representative images of GFP, FRET and FRET/GFP ratio during the course of STS followed by LPLI treatment. **E:** Sample records from time-lapse confocal measurements of GFP, FRET, and FRET/GFP ratio fluorescence intensities in cells treated with STS plus LPLI in the presence of wortmannin. Scale bar: 10  $\mu$ m. **F:** The quantitative time course of FRET/GFP ratios corresponding to the images in C–E. **G:** Co-immunoprecipitation with an anti-Akt antibody was used to pull-down Akt. Western blot for GSK-3 $\beta$  shows the amount of GSK-3 $\beta$  binding to Akt. Similar results were obtained from three independent experiments. [Color figure can be viewed in the online issue, which is available at [www.interscience.wiley.com](http://www.interscience.wiley.com).]

ratio of FRET/GFP are shown in Figure 5C–E. The quantitative analysis for the fluorescence intensity ratio of the FRET to GFP channel is shown in Figure 5F. The ratio remained stable without treatment, and started to have a slight decrease when STS was added. The decreased trend of the ratio was reversed after LPLI stimulation, and had a significant increase compared to its pre-STS treatment level, indicating the increased interaction between GFP-Akt and YFP-GSK-3 $\beta$ . However, the ratio decreased in the presence of wortmannin, indicating the decreased interaction between GFP-Akt and YFP-GSK-3 $\beta$ . In control cells, the ratio remained unchanged over 250 min (Fig. 5F). These results demonstrate that, activated Akt induced by LPLI could interact with and inactivate GSK-3 $\beta$  and this anti-apoptotic effect is dependent on PI3K activity.

In parallel, the experiment of co-immunoprecipitation was performed. The results display that the amount of Akt binding to GSK-3 $\beta$  increased markedly in response to LPLI (Fig. 5G). Taken together, these results demonstrate that, LPLI inhibits STS-induced apoptosis through inactivating GSK-3 $\beta$ , which is mediated by PI3K/Akt pathway.

#### LPLI inactivates GSK-3 $\beta$ /Bax pathway

Since we have demonstrated that LPLI could inactivate GSK-3 $\beta$  and suppress Bax activation, we expected to know how does

GSK-3 $\beta$  regulate Bax. In order to ascertain this, ASTC-a-1 cells were transiently co-transfected with GFP-Bax and YFP-GSK-3 $\beta$ , and stained with MitoTracker Red, followed by different treatments. The results show that in cells treated with STS, the emission in the GFP channel decreased, while the emission in the FRET channel and the ratio of the FRET/GFP channel increased (Fig. 6A), which was also confirmed by the quantitative analysis of FRET/GFP ratio (Fig. 6B), indicating the increased interaction between YFP-GSK-3 $\beta$  and GFP-Bax. However, in the cells treated with STS plus LPLI, the ratio was nearly unchanged as that of the control (Fig. 6B). These results suggest that LPLI protects cells from STS-induced apoptosis through inactivating GSK-3 $\beta$ /Bax pathway. This was further confirmed by the co-immunoprecipitation experiments (Fig. 6D). Interestingly, we found that Bax translocated from cytosol to mitochondria at about 3 h, with the increased interaction between GSK-3 $\beta$  and Bax (Fig. 6A,C), implying GSK-3 $\beta$  does promote Bax translocation by interacting with it during STS-induced apoptosis.

#### LPLI inhibits STS-induced cell apoptosis and Bax translocation through PI3K/Akt/GSK-3 $\beta$ pathway

The results in the present study show that LPLI could increase the cell viability significantly during STS-induced apoptosis

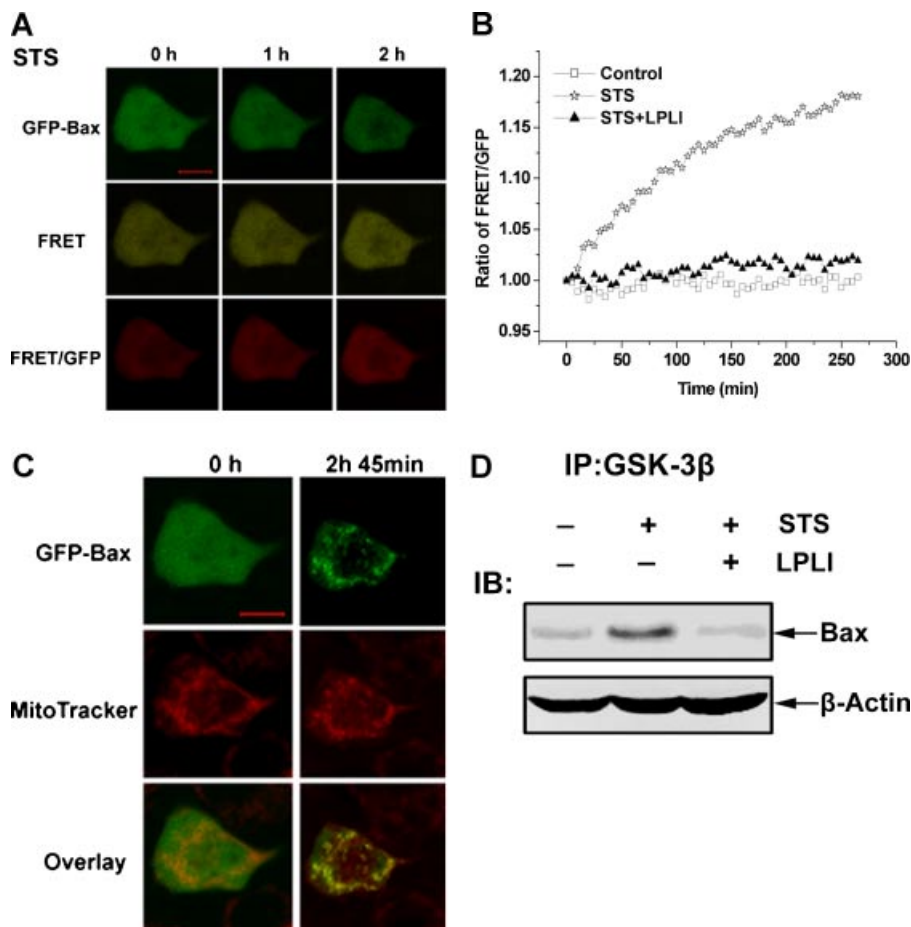


**Fig. 6.** Real-time monitoring of the interaction between GSK-3 $\beta$  and Bax. **A–C:** ASTC-a-1 cells co-transfected with YFP-GSK-3 $\beta$  and GFP-Bax were stained with Mito-Tracker, and then treated with 1  $\mu$ M STS or STS plus 1.2 J/cm<sup>2</sup> LPLI. **A:** Representative fluorescence image series of GFP, FRET, and FRET/GFP ratio of the cells treated with STS. **B:** Quantitative analysis of FRET/GFP ratio after various treatments. **C:** GFP-Bax translocates to mitochondria with the increased interaction of YFP-GSK-3 $\beta$  and GFP-Bax after STS treatment. **D:** Co-immunoprecipitation with an anti-GSK-3 $\beta$  antibody was used to pull-down GSK-3 $\beta$ . Western blot for Bax shows the amount of Bax binding to GSK-3 $\beta$ . Similar results were obtained from three independent experiments. [Color figure can be viewed in the online issue, which is available at [www.interscience.wiley.com](http://www.interscience.wiley.com).]

(Fig. 2). The following experiments were performed to detect the cell apoptosis by flow cytometric analysis after different treatments (Fig. 7A). The statistical analysis of cell apoptosis is shown in Figure 7B. Compared to the non-treated group, cell apoptosis increased obviously after STS stimulation, which was inhibited by LPLI or LiCl. While wortmannin could reverse the effect of LPLI for protection against STS-induced apoptosis. These results further demonstrate that LPLI protects cells from STS-induced apoptosis, which is dependent on the activation of PI3K/Akt and the inactivation of GSK-3 $\beta$ . Next, we wanted to know how important Bax is in STS-induced apoptosis. To address this question, siRNA constructs with specific sequences of Bax (siRNA-Bax) was transfected into ASTC-a-1 cells to block the expression of Bax. The result shows that siRNA-Bax did reduce the apoptosis level evidently (Fig. 7), suggesting Bax plays a critical role in STS-induced apoptosis.

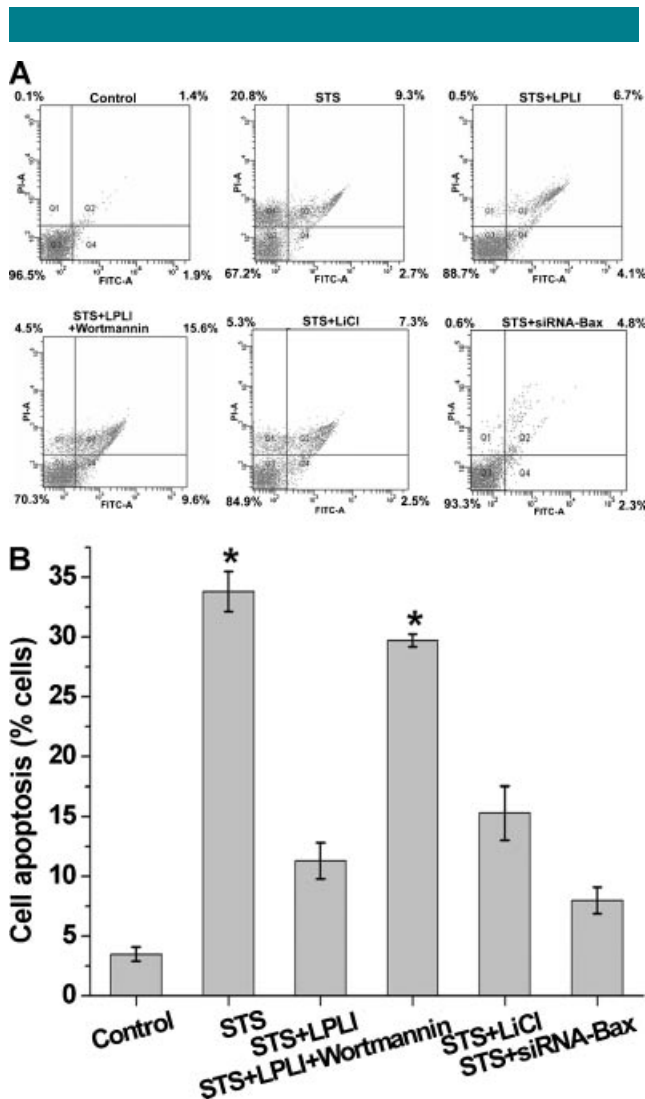


**Fig. 7.** Effects of LPLI, wortmannin, LiCl, and siRNA-Bax on STS-induced cell apoptosis and Bax translocation. **A:** FACS analysis of cell death under different experiment conditions. **B:** The percentage of apoptosis cells were used to calculate. Bars represent means  $\pm$  SEM from at least four independent experiments; \* $P < 0.05$ .

## Discussion

In the present study, the anti-apoptotic functions of LPLI and the underlying mechanisms are investigated. Our results contribute to the general idea that LPLI inhibits cell apoptosis through inactivating GSK-3 $\beta$ /Bax signaling pathway, which is mediated by the activation of PI3K/Akt: (1) LPLI-activated Akt (Fig. 3) interacts with and phosphorylates GSK-3 $\beta$  (Fig. 5C–G), leading to the inactivation of it (Fig. 5A,B). (2) STS induces apoptosis through activating GSK-3 $\beta$ /Bax pathway (Fig. 6), so inactivating GSK-3 $\beta$  by LPLI could suppress Bax translocation and apoptosis (Figs. 2 and 4). (3) Blockage of PI3K/Akt by wortmannin reserves the anti-apoptotic role of LPLI (Figs. 2–7).

LPLI is becoming a valuable means to therapy several diseases caused by cell apoptosis (Duan et al., 2001; Shefer et al., 2001; Zhang et al., 2008b). Several lines of evidence confirm that LPLI could protect cells from STS-induced apoptosis (Figs. 2 and 7). Akt serine/threonine protein kinases are critical for the regulation of fundamental cellular processes including cell proliferation and survival (Lawlor and Alessi, 2001). Our previous study has shown that LPLI could trigger the PI3K/Akt signaling pathway to promote cell proliferation in COS-7 cells (Zhang et al., 2009a). However, in the presence of apoptotic stress, can LPLI still activate Akt? If it can, what function does Akt perform in this process? FRET technology, a powerful tool that can spatio-temporally monitor cell events in physiological condition (Zhang et al., 2002, 2009b), was used to detect Akt activity in single living cell. We found that LPLI could activate Akt effectively even in the presence of STS (Fig. 3), and this anti-apoptotic role of LPLI is dependent on PI3K, because wortmannin could abolish the effect of LPLI (Fig. 2).

Bax, as a member of Bcl-2 family, is one of the most famous regulators in the apoptosis of mitochondrial pathway (Wei et al., 2001). Upon the apoptotic stimuli, it translocates from the cytosol to the mitochondria. To determine whether Bax is involved in LPLI-induced protection against apoptosis, real-time detection of GFP-Bax translocation was performed in living cell. The results show that Bax translocated to mitochondria after STS treatment (Fig. 4A,B), and importantly, this translocation was inhibited evidently by LPLI (Fig. 4C).

Next, we expect to know the hidden mechanism of LPLI inhibiting Bax translocation. Since we have proved that PI3K/Akt is activated during LPLI-induced protection against apoptosis (Figs. 2 and 3), we would like to know whether Akt is involved in LPLI inhibiting Bax translocation. And if it is, what is the relationship between Akt and Bax? Is there any other mediator involved in? GSK-3 $\beta$ , as a down-stream target of Akt (Cross et al., 1995), is an important activator of apoptosis (Bijur et al., 2000), which has been reported to trigger Bax translocation. Thus, we hypothesize that GSK-3 $\beta$  is the mediator between Akt and Bax during LPLI anti-apoptotic process.

To confirm this, we firstly detect the activity of GSK-3 $\beta$ . Our results show a clearly activation of GSK-3 $\beta$  by the accumulation of YFP-GSK-3 $\beta$  in the nucleus (Fig. 5A) and by the phosphorylation on Ser 9 after STS stimulation (Fig. 5B). Then, we should clarify what's the relationship among Akt, GSK-3 $\beta$ , and Bax, and whether they have direct interaction with each other. GSK-3 $\beta$  is known as a direct substrate of Akt. But the relationship between GSK-3 $\beta$  and Bax is complicated. There exist three opinions about GSK-3 $\beta$  regulating Bax translocation. Some researches have demonstrated that GSK-3 $\beta$  phosphorylates targets Mcl-1, and phosphorylated Mcl-1 is ubiquitinated and rapidly degraded, allowing Bim to activate Bax and MOMP (Letai, 2006). Some others show that GSK-3 $\beta$  markedly promoted p53-dependent conformational activation of Bax (Tan et al., 2005). Importantly, it has been reported that GSK-3 $\beta$  directly phosphorylates Bax and promotes its mitochondrial localization during cell apoptosis

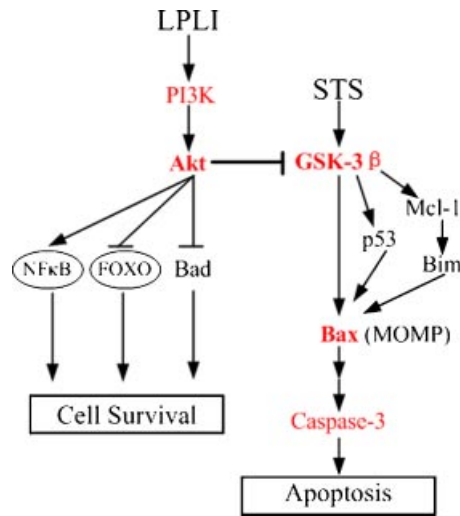


**Fig. 8.** A model of the signaling pathways of LPLI inhibiting STS-induced cell apoptosis. [Color figure can be viewed in the online issue, which is available at [www.interscience.wiley.com](http://www.interscience.wiley.com).]

(Linseman et al., 2004). To clarify it, FRET analysis and co-immunoprecipitation were used to detect the interaction between Akt and GSK-3 $\beta$ , as well as GSK-3 $\beta$  and Bax in single living cell. We found that Akt interacts with and inactivates GSK-3 $\beta$  after LPLI treatment (Fig. 5C–G). Also, GSK-3 $\beta$  interacts with and activates Bax directly, which was inhibited by LPLI (Fig. 6A,B). Interestingly, when cells were co-transfected with YFP-GSK-3 $\beta$  and GFP-Bax, the process of Bax translocation to mitochondria is accelerated (Fig. 6A,C) compared with the result of Figure 4B. In addition, Bax translocation induced by STS could be abolished by GSK-3 $\beta$  inhibitor LiCl (Fig. 4E). These results further confirm that GSK-3 $\beta$  interacts with Bax and promotes Bax translocation directly.

Finally, the flow cytometry was used to detect cell apoptosis directly on the statistical level (Fig. 7). LPLI inhibited more than a half of cell apoptosis induced by STS. While this anti-apoptotic effect was almost completely abolished by wortmannin, indicating the indispensability of PI3K/Akt pathway in LPLI-induced protection against apoptosis. GSK-3 $\beta$  inhibitor LiCl suppressed a large part of apoptosis, which suggested that GSK-3 $\beta$  is an essential signal after STS stimulation. Notably, LiCl did not reduce Bax translocation and apoptosis as much as LPLI treatment, implying that there may exist other regulators upstream of Bax translocation during STS-induced apoptosis. Meanwhile, LPLI-activated Akt has some other substrates (except for GSK-3 $\beta$ ) that can prevent Bax translocation. Therefore, one cannot rule out the possibility that other signals are associated with the anti-apoptotic effect of LPLI. Knocking down endogenous Bax by siRNA-Bax inhibits the most cell apoptosis, suggesting that Bax is the most important regulator for mitochondrial apoptosis induced by STS. Thus, the above results created a general idea that LPLI exerts its pro-survival function through selectively activating PI3K/Akt and suppressing GSK-3 $\beta$ /Bax pathway. Clearly, additional studies are required to fully delineate the anti-apoptotic mechanism of LPLI treatment.

In summary, the current study demonstrated that LPLI could protect cells against STS-induced apoptosis. We provided the first evidence that LPLI exerts its anti-apoptotic effect via activating PI3K/Akt signaling pathway. Specifically, Akt phosphorylates and inactivates GSK-3 $\beta$ , leading to the

inhibition of Bax translocation and caspase-3 activation (Fig. 8). The Akt-mediated inactivation of GSK-3 $\beta$ , as reflected by their increased interaction, plays an important role in inhibiting STS-induced cell apoptosis. Since the expression level and activity of GSK-3 $\beta$  were associated with neuron-degeneration, this raises the intriguing possibility that this PI3K/Akt/GSK-3 $\beta$ /Bax pathway plays a critical role in LPLI regulating neuronal cell survival as well as that of STS-treated ASTC-a-1 cells. The delineation of the signaling pathways involved in LPLI inhibiting STS-induced apoptosis will provide insight into establishing LPLI as a novel non-damage approach to neuron-protection therapy.

### Acknowledgments

This research is supported by the National Basic Research Program of China (2010CB732602), the Program for Changjiang Scholars and Innovative Research Team in University (IRT0829), and the National Natural Science Foundation of China (30870676 and 30870658). We thank Dr. Alexandra C. Newton (University of California, San Diego) for kindly providing Akt reporter plasmid, Dr. Thomas M. Badger (University of Arkansas for Medical Sciences, Little Rock, Arkansas) for kindly providing pEGFP-Akt, Dr. Miura, M. (RIKEN Brain Science Institute, Saitama, Japan) for kindly providing pSCAT3, Dr. John H. Kehrl (National Institutes of Health, Maryland, USA) for kindly providing pYFP-GSK-3 $\beta$ , Dr. Youle, R. J. (National Institutes of Health, Bethesda, USA) for kindly providing pGFP-Bax, Dr. Gotoh, Y. (University of Tokyo, Japan) for kindly providing pDsRed-Mit.

### Literature Cited

- Alessi DR, Andjelkovic M, Caudwell B, Cron P, Morrice N, Cohen P, Hemmings BA. 1996. Mechanism of activation of protein kinase B by insulin and IGF-1. *EMBO J* 15:6541–6551.
- Amano A, Miyagi K, Azuma T, Ishihara Y, Katsube S, Aoyama I, Saito I. 1994. Histological studies on the rheumatoid synovial membrane irradiated with a low energy laser. *Lasers Surg Med* 15:290–294.
- Ben-Dov N, Shefer G, Irintchev A, Wernig A, Oron U, Halevy O. 1999. Low-energy laser irradiation affects satellite cell proliferation and differentiation in vitro. *Biochim Biophys Acta* 1448:372–380.
- Bennett MR. 2002. Apoptosis in the cardiovascular system. *Heart (British Cardiac Society)* 87:480–487.
- Bijur GN, De Sarno P, Jope RS. 2000. Glycogen synthase kinase-3beta facilitates staurosporine- and heat shock-induced apoptosis. Protection by lithium. *J Biol Chem* 275:7583–7590.
- Bjorndal JM, Couppe C, Chow RT, Tuner J, Ljunggren EA. 2003. A systematic review of low level laser therapy with location-specific doses for pain from chronic joint disorders. *Aust J Physiother* 49:107–116.
- Bjorndal JM, Lopes-Martins RA, Iversen VV. 2006. A randomised, placebo controlled trial of low level laser therapy for activated Achilles tendinitis with microdialysis measurement of peritendinous prostaglandin E2 concentrations. *Br J Sports Medicine* 40:76–80; discussion 76–80.
- Brunet A, Bonni A, Zigmond MJ, Lin MZ, Juo P, Hu LS, Anderson MJ, Arden KC, Blenis J, Greenberg ME. 1999. Akt promotes cell survival by phosphorylating and inhibiting a Forkhead transcription factor. *Cell* 96:857–868.
- Cardone MH, Roy N, Stennicke HR, Salvesen GS, Franke TF, Stanbridge E, Frisch S, Reed JC. 1998. Regulation of cell death protease caspase-9 by phosphorylation. *Science (New York, NY)* 282:1318–1321.
- Chen RH, Su YH, Chuang RL, Chang TY. 1998. Suppression of transforming growth factor-beta-induced apoptosis through a phosphatidylinositol 3-kinase/Akt-dependent pathway. *Oncogene* 17:1959–1968.
- Chow RT, Barnsley L. 2005. Systematic review of the literature of low-level laser therapy (LLLT) in the management of neck pain. *Lasers Surg Med* 37:46–52.
- Conlan MJ, Rapley JW, Cobb CM. 1996. Biostimulation of wound healing by low-energy laser irradiation. A review. *J Clin Periodontol* 23:492–496.
- Cross DA, Alessi DR, Cohen P, Andjelkovic M, Hemmings BA. 1995. Inhibition of glycogen synthase kinase-3 by insulin mediated by protein kinase B. *Nature* 378:785–789.
- Cross TG, Scheel-Toellner D, Henriquez NV, Deacon E, Salmon M, Lord JM. 2000. Serine/threonine protein kinases and apoptosis. *Exp Cell Res* 256:34–41.
- Crowder RJ, Freeman RS. 1998. Phosphatidylinositol 3-kinase and Akt protein kinase are necessary and sufficient for the survival of nerve growth factor-dependent sympathetic neurons. *J Neurosci* 18:2933–2943.
- Datta SR, Dudek H, Tao X, Masters S, Fu H, Gotoh Y, Greenberg ME. 1997. Akt phosphorylation of BAD couples survival signals to the cell-intrinsic death machinery. *Cell* 91:231–241.
- Deas O, Dumont C, MacFarlane M, Rouleau M, Hebib C, Harper F, Hirsch F, Charpentier B, Cohen GM, Senik A. 1998. Caspase-independent cell death induced by anti-CD2 or staurosporine in activated human peripheral T lymphocytes. *J Immunol* 161:3375–3383.
- Duan R, Liu TC, Li Y, Guo H, Yao LB. 2001. Signal transduction pathways involved in low intensity He-Ne laser-induced respiratory burst in bovine neutrophils: A potential mechanism of low intensity laser biostimulation. *Lasers Surg Med* 29:174–178.
- Dudek H, Datta SR, Franke TF, Birnbaum MJ, Yao R, Cooper GM, Segal RA, Kaplan DR, Greenberg ME. 1997. Regulation of neuronal survival by the serine-threonine protein kinase Akt. *Science (New York, NY)* 275:661–665.

- Earnshaw WC, Martins LM, Kaufmann SH. 1999. Mammalian caspases: Structure, activation, substrates, and functions during apoptosis. *Annu Rev Biochem* 68:383–424.
- Gao X, Chen T, Xing D, Wang F, Pei Y, Wei X. 2006. Single cell analysis of PKC activation during proliferation and apoptosis induced by laser irradiation. *J Cell Physiol* 206:441–448.
- He L, Simmen FA, Mehendale HM, Ronis MJ, Badger TM. 2006. Chronic ethanol intake impairs insulin signaling in rats by disrupting Akt association with the cell membrane. Role of TRB3 in inhibition of Akt/protein kinase B activation. *J Biol Chem* 281:11126–11134.
- Hirschl M, Katzenschlager R, Francesconi C, Kundl M. 2004. Low level laser therapy in primary Raynaud's phenomenon—Results of a placebo controlled, double blind intervention study. *J Rheumatol* 31:2408–2412.
- Hsu YT, Wolter KG, Youle RJ. 1997. Cytosol-to-membrane redistribution of Bax and Bcl-X(L) during apoptosis. *Proc Natl Acad Sci USA* 94:3668–3672.
- Kang PM, Izumo S. 2003. Apoptosis in heart: Basic mechanisms and implications in cardiovascular diseases. *Trends Mol Med* 9:177–182.
- Kauffmann-Zeh A, Rodriguez-Viciana P, Ulrich E, Gilbert C, Coffey P, Downward J, Evan G. 1997. Suppression of c-Myc-induced apoptosis by Ras signalling through PI(3)K and PKB. *Nature* 385:544–548.
- Kennedy SG, Wagner AJ, Conzen SD, Jordan J, Bellacosa A, Tschlis PN, Hay N. 1997. The PI 3-kinase/Akt signaling pathway delivers an anti-apoptotic signal. *Genes Dev* 11:701–713.
- Khawaja A, Rodriguez-Viciana P, Wennstrom A, Warne PH, Downward J. 1997. Matrix adhesion and Ras transformation both activate a phosphoinositide 3-OH kinase and protein kinase B/Akt cellular survival pathway. *EMBO J* 16:2783–2793.
- Kim AH, Khursigara G, Sun X, Franke TF, Chao MV. 2001. Akt phosphorylates and negatively regulates apoptosis signal-regulating kinase 1. *Mol Cell Biol* 21:893–901.
- Kunkel MT, Ni Q, Tsien RY, Zhang J, Newton AC. 2005. Spatio-temporal dynamics of protein kinase B/Akt signaling revealed by a genetically encoded fluorescent reporter. *J Biol Chem* 280:5581–5587.
- Lawlor MA, Alessi DR. 2001. PKB/Akt: A key mediator of cell proliferation, survival and insulin responses? *J Cell Sci* 114:2903–2910.
- Letai A. 2006. Growth factor withdrawal and apoptosis: The middle game. *Mol Cell* 21:728–730.
- Linseman DA, Butts BD, Precht TA, Phelps RA, Le SS, Laessig TA, Bouchard RJ, Florez-McClure ML, Heidenreich KA. 2004. Glycogen synthase kinase-3beta phosphorylates Bax and promotes its mitochondrial localization during neuronal apoptosis. *J Neurosci* 24:9993–10002.
- Mizutani K, Musya Y, Wakae K, Kobayashi T, Tobe M, Taira K, Harada T. 2004. A clinical study on serum prostaglandin E2 with low-level laser therapy. *Photomed Laser Surg* 22:537–539.
- Mookherjee P, Quintanilla R, Roh MS, Zmijewska AA, Jope RS, Johnson GV. 2007. Mitochondrial-targeted active Akt protects SH-SY5Y neuroblastoma cells from staurosporine-induced apoptotic cell death. *J Cell Biochem* 102:196–210.
- Nechushtan A, Smith CL, Hsu YT, Youle RJ. 1999. Conformation of the Bax C-terminus regulates subcellular location and cell death. *EMBO J* 18:2330–2341.
- Ozes ON, Mayo LD, Gustin JA, Pfeffer SR, Pfeffer LM, Donner DB. 1999. NF-kappaB activation by tumour necrosis factor requires the Akt serine-threonine kinase. *Nature* 401:82–85.
- Qu L, Huang S, Baltzis D, Rivas-Estilla AM, Pluquet O, Hatzoglou M, Koumenis C, Taya Y, Yoshimura A, Koromilas AE. 2004. Endoplasmic reticulum stress induces p53 cytoplasmic localization and prevents p53-dependent apoptosis by a pathway involving glycogen synthase kinase-3beta. *Genes Dev* 18:261–277.
- Schindl A, Schindl M, Pernerstorfer-Schon H, Kerschman K, Knobler R, Schindl L. 1999. Diabetic neuropathic foot ulcer: Successful treatment by low-intensity laser therapy. *Dermatology (Basel, Switzerland)* 198:314–316.
- Shefer G, Oron U, Irintchev A, Wernig A, Halevy O. 2001. Skeletal muscle cell activation by low-energy laser irradiation: A role for the MAPK/ERK pathway. *J Cell Physiol* 187:73–80.
- Shefer G, Partridge TA, Heslop L, Gross JG, Oron U, Halevy O. 2002. Low-energy laser irradiation promotes the survival and cell cycle entry of skeletal muscle satellite cells. *J Cell Sci* 115:1461–1469.
- Shi CS, Huang NN, Harrison K, Han SB, Kehrl JH. 2006. The mitogen-activated protein kinase kinase kinase GSK3R positively regulates canonical and noncanonical Wnt signaling in B lymphocytes. *Mol Cell Biol* 26:6511–6521.
- Silveira PC, Silva LA, Fraga DB, Freitas TP, Streck EL, Pinho R. 2009. Evaluation of mitochondrial respiratory chain activity in muscle healing by low-level laser therapy. *J Photochem Photobiol B* 95:89–92.
- Stepczynska A, Lauber K, Engels IH, Janssen O, Kabelitz D, Wesselborg S, Schulze-Osthoff K. 2001. Staurosporine and conventional anticancer drugs induce overlapping, yet distinct pathways of apoptosis and caspase activation. *Oncogene* 20:1193–1202.
- Tafani M, Cohn JA, Karpnich NO, Rothman RJ, Russo MA, Farber JL. 2002. Regulation of intracellular pH mediates Bax activation in HeLa cells treated with staurosporine or tumor necrosis factor-alpha. *J Biol Chem* 277:49569–49576.
- Tafur J, Mills PJ. 2008. Low-intensity light therapy: Exploring the role of redox mechanisms. *Photomed Laser Surg* 26:323–328.
- Takemoto K, Nagai T, Miyawaki A, Miura M. 2003. Spatio-temporal activation of caspase revealed by indicator that is insensitive to environmental effects. *J Cell Biol* 160:235–243.
- Tan J, Zhuang L, Leong HS, Iyer NG, Liu ET, Yu Q. 2005. Pharmacologic modulation of glycogen synthase kinase-3beta promotes p53-dependent apoptosis through a direct Bax-mediated mitochondrial pathway in colorectal cancer cells. *Cancer Res* 65:9012–9020.
- Tsuruta F, Masuyama N, Gotoh Y. 2002. The phosphatidylinositol 3-kinase (PI3K)-Akt pathway suppresses Bax translocation to mitochondria. *J Biol Chem* 277:14040–14047.
- Watcharasil P, Bijur GN, Song L, Zhu J, Chen X, Jope RS. 2003. Glycogen synthase kinase-3beta (GSK3beta) binds to and promotes the actions of p53. *J Biol Chem* 278:48872–48879.
- Wei MC, Zong WX, Cheng EH, Lindsten T, Panoutsakopoulou V, Ross AJ, Roth KA, MacGregor GR, Thompson CB, Korsmeyer SJ. 2001. Proapoptotic BAX and BAK: A requisite gateway to mitochondrial dysfunction and death. *Science (New York, NY)* 292:727–730.
- Yamaguchi A, Tamatani M, Matsuzaki H, Namikawa K, Kiyama H, Vitek MP, Mitsuda N, Tohyama M. 2001. Akt activation protects hippocampal neurons from apoptosis by inhibiting transcriptional activity of p53. *J Biol Chem* 276:5256–5264.
- Yu HS, Chang KL, Yu CL, Chen JW, Chen GS. 1996. Low-energy helium-neon laser irradiation stimulates interleukin-1 alpha and interleukin-8 release from cultured human keratinocytes. *J Invest Dermatol* 107:593–596.
- Zhang J, Campbell RE, Ting AY, Tsien RY. 2002. Creating new fluorescent probes for cell biology. *Nat Rev* 3:906–918.
- Zhang J, Xing D, Gao X. 2008a. Low-power laser irradiation activates Src tyrosine kinase through reactive oxygen species-mediated signaling pathway. *J Cell Physiol* 217:518–528.
- Zhang L, Xing D, Zhu D, Chen Q. 2008b. Low-power laser irradiation inhibiting Abeta25-35-induced PC12 cell apoptosis via PKC activation. *Cell Physiol Biochem* 22:215–222.
- Zhang L, Xing D, Gao X, Wu S. 2009a. Low-power laser irradiation promotes cell proliferation by activating PI3K/Akt pathway. *J Cell Physiol* 219:553–562.
- Zhang Y, Xing D, Liu L. 2009b. PUVA promotes Bax translocation by both directly interacting with Bax and competitive binding to Bcl-XL during UV-induced apoptosis. *Mol Biol Cell* 20:3077–3087.